CHAPTER XXXI

FROM MODERN HUMANS TO SPY ANCESTORS? COMPARISON OF THE LOCOMOTION OF ANATOMICALLY MODERN HUMANS AND NEANDERTALS (SPY II): A FEASIBILITY STUDY

Tara CHAPMAN, Fedor MOISEEV,
Stéphane LOURYAN, Marcel ROOZE & Serge VAN SINT JAN

Abstract

*This chapter presents a feasibility study to analyse whether Neandertals had a similar bipedal gait to anatomically modern humans. CT scans of originals from Spy II and casts from Kebara 2 and Neandertal 1 were analysed to obtain three-dimensional (3D) bone morphology from medical imaging data. Skeletal landmarks were virtually palpated on each available bone. From these landmarks spatial transformations between Neandertal 1, Kebara 2 and Spy II were performed to reconstruct a 3D skeletal model of two lower limbs and a pelvis. An in-vivo human motion squatting model was then registered to the reconstructed 3D models, including a 6 DOFs mechanism at both the knee and ankle joint. The same method was applied on the skeleton of a bonobo (*Pan paniscus*) to test and validate the adopted experimental paradigm. Results were visualised via a computer graphics output. Early results seem to show that Neandertals had similar knee joint morphology to modern day humans and bipedal gait is likely to be similar as no obvious difference could be found in their respective motion representation. The bonobo data shows major differences. The entire data processing and data visualisation pipeline was implemented in a customised software interface called lhpFusionBox.*

INTRODUCTION

Context

Hominids are distinct from other primates in having an erect bipedal posture and a striding gait. Evidence for bipedal gait has been proposed in early hominids at least as far back as 3.5 million years (Carrier *et al.*, 1984; Richmond & Jungers, 2008). Analysis of fossil hominid locomotion has been inferred by analysis of the external morphological surface, cortical bone distribution, limb proportions and body mass (Trinkaus, 1983; Trinkaus *et al.*, 1998, 1999; Steudel-Numbers & Tilkens, 2004; Ruff, 2009). The use of computing technologies (ICT) to study locomotion, gait and the musculoskeletal system has gained important ground in the clinical setting in the last few decades (Van Sint Jan, 2005). Similar technologies are becoming increasingly popular in palaeoanthropological reconstructions of Neandertal fossil locomotion, utilising inverse kinematics, evolutionary robot-

ics and the combination of Neandertal skeletal data with kinematic data on primates and anatomically modern humans (Miller & Gross, 1998; Polk, 2004; Sellers *et al.*, 2004; Steudel-Numbers & Tilkens, 2004; Gruss, 2007).

There has been a long standing debate on whether Neandertals should be classified as belonging to the species *Homo sapiens*, "*Homo sapiens neanderthalensis*" or as a separate species "*Homo neanderthalensis*" (Trinkaus & Shipman, 1992; Tattersall & Schwartz, 2007). This debate has also included ideas on whether or not Neandertals had a similar bipedal gait to early and modern humans.

Early to present day ideas of Neandertal gait

Following publication of Marcellin Boule's (Boule, 1911, 1912, 1913) monographs on the anatomy of the La Chapelle-aux-Saints skeletal material, early ideas of Neandertals were that of ape-like, hairy creatures, slouched and

bent-kneed with "a less perfect bipedal or upright carriage than in modern Man" (Boule & Vallois, 1957: 252). The geologist Maximin Lohest who discovered the Spy fossils with Marcel De Puydt (for further information see Semal *et al.*, volume 1: chapter II) depicted a similar picture of Neandertals in the 1880s, although this drawing has not previously been published (Figure 1). These ideas generally persisted until the late 1950s when researchers criticised early interpretations and found that the skeletal morphology of Neandertals was fully compatible with the erect posture and bipedality of modern day humans (Trinkaus, 1985). Recent studies have further confirmed that the Neandertal lower limb skeletal morphology seems to have a locomotive pattern within human ranges of variation and a bipedal gait which is likely to be indistinguishable from that of anatomically modern humans (Trinkaus, 1983, 1985; Trinkaus & Ruff, 1989).

Figure 1. The first drawing of Neandertal man with bent knees and crouched stance, as depicted by Lohest in the 1880s (published with kind permission of the Royal Belgian Institute of Natural Sciences).

Available Neandertal fossils

The Spy II skeletal morphology is similar to other Neandertal skeletal material, exhibiting a robust postcranial skeleton, large diaphyseal diameters of the tibia and femur relative to length, rounded shafts of the tibia and femur, bowing of femur, retroverted tibia and robust calcaneus (Fraipont & Lohest, 1886, 1887; Hrdlička, 1930; Trinkaus & Ruff, 1989). Neandertal skeletal morphology is commonly viewed as "hyperpolar" and the robustness of the skeleton, relatively short stature and low crural indices, follow Bergmann's and Allen's rule of a cold-climate adaptation, traits also found in cold-climate adapted modern humans (Trinkaus, 1981; Weaver, 2003). The differential skeletal morphology has also been variously interpreted as an adaptation for frequently elevated levels of bio-mechanical stress, consistent with higher mechanical loads or simply as genetic baggage (Trinkaus, 1981; Trinkaus & Ruff, 1989; Ruff *et al.*, 1993; Trinkaus *et al.*, 1994, 1999; Weaver, 2003). The skeletal components utilised within this study have recently been attributed to the Spy II skeleton and we refer to those skeletal elements as Spy II throughout the text (Hrdlička, 1930; Ben-Itzhak *et al.*, 1988; although see Rougier *et al.*, this volume: chapter XIX for a more complete review of the various attributions).

As with other early hominid skeletal remains, the remains of the Spy II skeleton are not complete and are not sufficient to study potential locomotion patterns. Sawyer & Maley (2005) previously reconstructed a complete articulated Neandertal skeleton based on differential fossil remains although this skeleton is currently not available in digitised form. Therefore the first aim of our study was to reconstruct a complete lower limb skeleton for the Spy II individual, which included a pelvis and two lower limbs. In summary (more details are given below), the method implemented in this paper used mirroring techniques to duplicate heterolateral counterparts of available Spy II bones. Missing bone elements were obtained using a newly-developed double-scaling method utilising the Kebara 2 and Neandertal 1 remains. This reconstruction was performed alongside a validated registration method to keep track of the accuracy of the various geometrical transformations in which

models were processed. This validation procedure also enabled the quantification of morphological difference between bones.

Hypothesis on Neandertal locomotion

Previous studies have suggested that Neandertals had a similar gait to modern humans (Trinkaus, 1983, 1985; Trinkaus & Ruff, 1989). The Kebara 2 pelvis represents the most complete Neandertal pelvis found to date and was used in order to have a complete lower limb model of a Neandertal skeleton. The pelvis does not significantly differ in size from anatomically modern humans although there are several morphological differences. Similar to other Neandertal specimens, there is an unusually wide sub-pubic angle (110°) and a different orientation of the acetabulae (Rak & Arensburg, 1987; Rak, 1991). Rak & Arensburg (1987) have suggested these differences may be attributable to a difference in locomotion and posture-related mechanics. However, similar to other researchers on the lower limb (Trinkaus, 1983, 1985; Trinkaus & Ruff, 1989), we will start from the null hypothesis: Neandertals had a similar bipedal gait to anatomically modern humans.

This feasibility study is based solely on the morphological aspect of the joint surface and related kinematics although we started with the assumption that Spy II and Kebara 2 had muscle and ligament recruitment similar to anatomically modern humans. This was the methodology previously adopted when analysing the fossil hominid AL 288-1 (Wang *et al.*, 2004; Sellers *et al.*, 2005).

The above hypotheses allowed us to apply a recently available method which is used in in-vivo and clinical settings (Sholukha *et al.*, 2006). The method enables 6 degrees-of-freedom (DOFs) joint kinematics and gait motion data to be scaled to individual three-dimensional (3D) bone models. The results of this registration include computer graphics visualisations which gave an initial qualitative impression to determine whether joint behaviour appears to be physiological or not. The use of conventional motion representation further enabled qualitative motion comparison (Van Sint Jan *et al.*, 2003).

METHODS AND RELATED RESULTS

Reconstruction of Neandertal 3D morphological model

The aim of this section was to create a complete lower limb skeleton. As the Spy II remains do not include any iliac bones, the Neandertal 1 and Kebara 2 remains were used to achieve this goal using the protocol described below. Earlier studies of the Spy II fossil material designated this specimen as a male (Fraipont & Lohest, 1886, 1887; Hrdlička, 1930; Ben-Itzhak *et al.*, 1988), although for further discussion on this, see Rougier *et al.* (this volume: chapter XIX). The Spy II specimen was recently dated as being approximately 36,000 years old (Semal *et al.*, 2009). The Kebara 2 pelvis has also been designated as male, with an estimated age of 50 - 55,000 years old (Bar-Yosef *et al.*, 1992). The Neandertal 1 skeleton was recently dated as being approximately 40,000 years old although the sex of the skeleton is not detailed (Schmitz *et al.*, 2002). Casts and originals of bones utilised were obtained from the Royal Belgian Institute of Natural Sciences and included: Spy II skeleton – original bones (right femur (Spy 8), left patella (Spy 19), left tibia (Spy 9), left fibula - distal 4th (Spy 26B), left calcaneus (Spy 17), left talus (Spy 18)), Neandertal 1 skeleton – cast (left iliac bone, left femur) and Kebara 2 skeleton – cast (right iliac bone).

CT scans of Spy II were utilised with permission from the Royal Belgian Institute of Natural Sciences (Balzeau *et al.*, this volume: chapter XXII). All casts and bones were processed by medical imaging (Computerised Tomography or CT) at the Radiology Department of the ULB Erasmus Hospital or at the Laboratory of Anatomy, Biomechanics and Organogenesis (LABO), ULB. Imaging settings are available in ST1. CT image stacks were imported into a software programme to perform segmentation (AMIRA®). On each bone, a semi-automated extraction of bone information was performed on the CT data and a 3D geometrical model was obtained. This procedure creates a faithful and accurate representation, although 3D bone models generated from these types of systems usually include a very high number of facets (typically, several hundreds of thou-

sands) which require a large memory capacity. Bone models have to remain usable to allow real time simulation using standard computer graphics hardware, therefore all available models were reduced to a manageable size. Femoral, tibial and iliac bones were decimated, i.e. reduced, to 150,000 and 80,000 facets (ST2), while smaller bones were decimated to 50,000 facets (Van Sint Jan, 2005).

All bone models were then stored in STL file format for further use. Model decimation and smoothing can reduce bone surface accuracy if performed too drastically and useful bone detail could be smoothed out (Van Sint Jan, 2005). To avoid these problems, the original bones and casts were used in comparison with the 3D models as a visual qualitative assessment to ensure that 3D models were anatomically realistic. After reconstruction and decimation, all available 3D bone models were imported into a customised software interface called lhpFusion-

Box. The latter software was used for the remainder of the data processing pipeline.

lhpFusionBox is a program which was originally designed for biomechanical and clinical studies relating to the musculoskeletal system of modern humans although has recently been adapted for palaeoanthropological purposes (Van Sint Jan *et al.*, 2006; Viceconti *et al.*, 2007a). The design makes it possible to import, fuse, and store within the digital library, almost any type of biomedical data, including medical images in DICOM format, gait analysis data and finite element analysis results (Viceconti *et al.*, 2007b).

Palpation of anatomical landmarks

Skeletal landmarks are particular bony features that are recognisable at the surface of bones or 3D bone models. Palpation of bone anatomical landmarks (ALs) enables the measurement of morphological features and the compar-
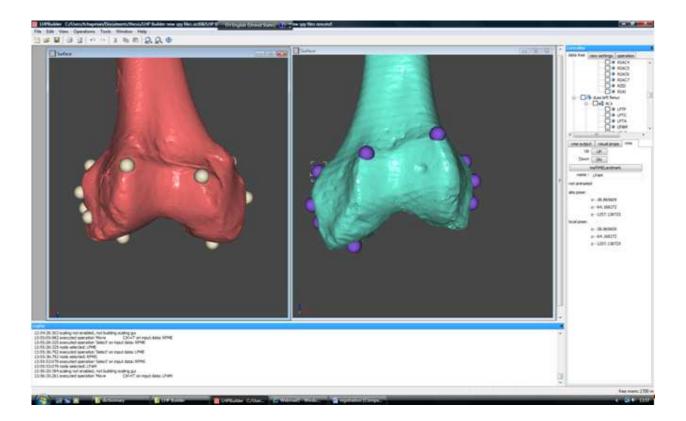

Figure 2. Virtual palpation of ALs.
Two femur bone models are displayed in two separate surface viewers within the lhpFusionBox environment. Left: Spy II femur; Right: Neandertal 1 femur. Coloured spheres indicate AL location selected by the operator using virtual palpation. The data tree on the right shows the organisation of the imported data within lhpFusionBox.

ison of various bones with each other, as well as more complex operations such as spatial registration. Strict AL definitions (ST3) (Van Sint Jan, 2007) were used to guarantee reproducibility as discrepancies during AL palpation can lead to unsatisfactory motion simulation.

The use of several viewers in lhpFusion-Box allowed a side by side analysis of comparative bones so that palpated landmarks on similar skeletal elements can be verified and checked, i.e. the Neandertal 1 femur and Spy II femur were processed together to ensure that palpated ALs matched (Figure 2). After virtual palpation, 3D model anatomical accuracy and selected AL location were subsequently examined by senior members of LABO for further validation.

Several standardised ALs were not able to be palpated on available specimens due to localised damage. The greater trochanter is missing on the Spy II femur and was not able to be palpated. The distal lateral condyle was slightly damaged in the left Neandertal 1 femur and the most distal point of the lateral condyle was unavailable. Two ALs of the acetabulum were not clearly visible on the Neandertal 1 iliac bone. All other bones were relatively complete with the exception of the Spy II fibula, which was only the distal 4th. The only AL that could be palpated on this bone was the apex of the lateral malleolus (ST3). After virtual palpation, locations of standardised ALs (ST3) were available for further registration purposes (Van Sint Jan, 2007).

Generation of 3D models of missing bones by mirroring

Ancient hominid fossils skeletons are rarely complete and frequently only one side is found. lhpFusionBox was adapted to allow mirroring of available bone models simultaneously with their previously-located ALs (ST3 and Figure 3). In this way we were able to create a complete dataset of 3D bone models required for further modelling of the lower limbs.

Scaling Kebara 2 to Spy II dimensions by double registration

The three Neandertal specimens (Spy II, Neandertal 1 and Kebara 2) enabled the recon-

struction of two entire lower limbs, including the pelvis. The Kebara 2 iliac bone was used as it is the most complete Neandertal pelvis available and the Spy II remains do not include iliac bones. The Neandertal 1 pelvis and femur were used as an intermediate scaling stage as there are no common bone elements between the Spy II and Kebara 2 skeletons (Figure 3). The Neandertal 1 and Spy II remains demonstrate a similar robusticity (Trinkaus & Ruff, 1989).

Model scaling was performed in two stages using spatial data registration from the previously located ALs. The first scaling stage scaled the Kebara 2 iliac bone to the Neandertal 1 iliac bone. The second stage scaled the result of the first stage to the Spy II femoral dimensions. Scaling procedure was based on standard singular value decomposition, or SVD, algorithms (Horn, 1987; Challis, 1995; Van Sint Jan *et al.*, 2002). Registration was performed using similarity scaling which rotates, translates and scales the object but does not change the shape (i.e. inhomogeneous scaling). The latter transformation would have altered the morphology of the scaled bones and was therefore unacceptable within the frame of this study. Accuracy of the transformation was given by the root mean square (RMS) error of the various ALs processed by the algorithm (Challis, 1995).

The dispersion of ALs between the Kebara 2 and Neandertal 1 iliac bones led to a small RMS error of 10.8 mm. Scaling of the Kebara 2 iliac bone to Spy II dimensions was performed using the available femurs as an intermediate scaling. Results of this transformation led to an RMS error of 6.0 mm. Previous authors have reported various methods which allow the registration of one particular object to another: for example using least squares methods or SVD algorithms (Horn, 1987; Challis, 1995). This study used least squares algorithms to develop the new scaling procedure which registered the Kebara 2 pelvis to the Spy II femur via the Neandertal 1 femur (further details of the method of the SVD algorithm can be found in Challis, 1995). The results were the Kebara 2 iliac bones scaled to the Spy II morphology (Figure 3). The scaled bone segments were then ready to be fused to joint kinematics and motion data.
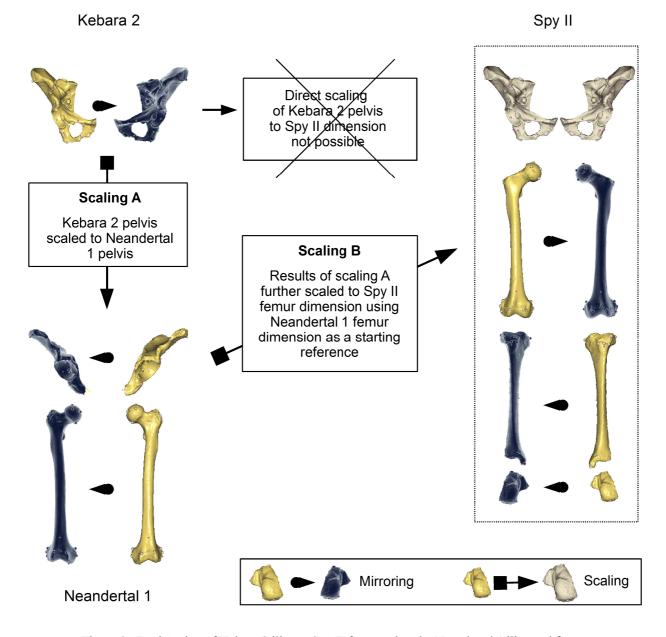
Figure 3. Registration of Kebara 2 iliac to Spy II femur using the Neandertal 1 iliac and femur.
There was no direct transformation possible between Kebara 2 and Spy II. A: The first stage registered the Kebara 2 iliac to the Neandertal 1 iliac; B: The second stage scaled the result of the first stage to the Neandertal 1 femur and then to the Spy II femur, to further register the Kebara 2 pelvis to Spy II dimensions.

Motion reconstruction and analysis

Advanced registration to joint kinematics and motion analysis data

This section describes how motion data were fused to the above results to analyse potential Spy II kinematics. Classical motion modelling, registering bone morphology (i.e. 3D bone models) to given tasks using AL spatial location, reduces the number of degrees-of-freedom (DOFs) available in the model (for example, by making the joint motion centre fixed). This procedure has the advantage of avoiding noise artefacts during the visual display which are due to limitations of the current motion analysis system (Sholukha *et al.*, 2006). This approach is acceptable for gross joint motion visualisation, but not for the advanced analysis of detailed joint behaviour that we wanted to achieve in this study.

Therefore the advanced registration method developed by Sholukha *et al.* (2006) was adopted in this study.

In summary (further details of the method can be found in Sholukha *et al.*, 2006), the new approach proposes a 6 DOFs (3 rotations and 3 translations) mechanism for the knee and ankle joint kinematics. These mechanisms can be synchronised to motion data taken from volunteers performing motion (e.g. walking, squatting) via registration algorithms using the available spatial-temporal information. The final model then demonstrates complex joint behaviour; e.g. the rolling-gliding phenomenon of the femoral condyles during knee flexion (Kapandji, 1985; Van Sint Jan *et al.*, 2002) based on standard singular value decomposition (SVD) algorithms.

The final goal of this study was to apply a particular motion pattern, obtained from an anatomically modern human, to the above skeletal elements to determine if the results support the initial hypothesis that bone morphology and joint surfaces of Neandertals demonstrate similar motion patterns to anatomically modern humans. The adoption of a method that allows for the integration of 6 DOFs in the joint was therefore of vital importance to accurately analyse gliding of the joint surfaces during motion and detection, e.g. to analyse whether there are unrealistic bone collisions or joint dislocations due to incompatible joint surfaces within a given motion pattern.

Within this study, we registered the previously scaled skeletal segments (see section on "Reconstruction of Neandertal 3D morphological model") to the available kinematics data. The latter data included the description of 3D trajectories of ALs during analysed motions. In this study, ALs manually palpated during in-vivo motion analysis were the same as the virtually palpated ALs on the Neandertal specimens. This facilitated the fusion (i.e. registration of heterogeneous data) of morphological and motion data. The dispersion of ALs between the modern human data and the reconstructed Neandertal limbs were then evaluated via similarity scaling. RMS errors ranged between 0.4 mm and 17.7 mm (Table 1). The registration was performed via rigid scaling, which includes translation and rotation of data, but does not scale the data. RMS errors for rigid scaling ranged between 2.1 mm and 17.6 mm (Table 1).

Models that are in 3D require at least three ALs to perform registration. The available motion data relating to the anatomically modern human talus and patella does not currently include 3 manually palpated ALs. Therefore, corresponding fossil bones were not registered and missing fossil models were substituted with their modern equivalent. Registration was implemented using SVD procedures (similar to the ones used in the above scaling process). Final registration led to the availability of a full lower limb for further behavioural analysis which was reconstructed mainly from Neandertal remains (Figure 4).

The visualisation of the reconstructed Neandertal skeleton (Figure 4) and associated RMS errors (Table 1) indicated that the presented scaling paradigm was satisfactory. RMS errors (Table 1) were relatively small which verified the fact that Neandertal skeletal and joint morphology is similar to that of anatomically modern humans.

Neandertal Model	AMH Model	Similarity Left bone	Similarity Right bone	Rigid Left bone	Rigid Right bone
Spy 8 (Spy II) femur	femur	7.9	6.5	14.4	13.1
Spy 9 (Spy II) tibia	tibia	5.1	8.0	15.8	16.5
Spy 17 (Spy II) calcaneus	calcaneus	0.4	0.5	2.1	2.5
Kebara 2 iliac bone prior to scaling	iliac	17.7	16.3	17.6	16.2
Kebara 2 iliac bone scaled to Spy femur	iliac	14.4	15.6	14.4	15.5

Table 1. RMS error (in mm) between anatomically modern human (AMH) and Neandertal models. Although left and right fossil models were identical in proportion (due to mirroring, see above description), different RMS errors were obtained for the left and right sides because anatomically modern human bones were not mirrored.
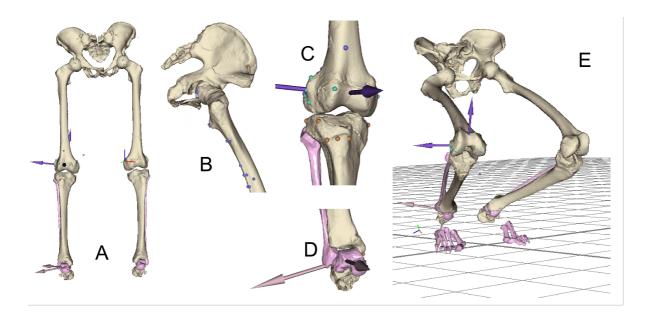
Figure 4. Visualisation of final registration of Neandertal data to motion data. A: full skeleton; B: view on the hip joint; C: detail on the knee joint; D: detail on the ankle joint; E: Neandertal skeleton during a squat movement. Bones in pink are anatomically modern humans (AMH) and bones in white are Neandertal.

*Application of the method to bonobo (*Pan paniscus*) skeleton*

To test the validity of the above method, we applied the same procedure to a 3D skeletal model of a bonobo. The same null hypothesis was also used: *Bonobos have a similar bipedal gait to anatomically modern humans.* Whilst this assumption is of course nonsensical (bonobos rarely engaging in bipedal gait), it was performed to verify the robustness of our method. The specimen used in this study was an alpha-male (age: 29 y.o., weight: 60.0 kg, foot length: 25.5 cm) who died in 2000 of a natural death (Vereecke *et al.*, 2005).

With the same methodology as described above for the Neandertals, the right bonobo tibia, fibula and femur were registered to the available kinematics data. ALs manually palpated during motion analysis were the same as virtually palpated ALs on the bonobo specimens. The dispersion of ALs between the anatomically modern human data and the bonobo data was then evaluated using RMS errors. This process demonstrated large RMS errors in the bonobo data (right bonobo tibia and fibula: 27.8 mm rigid registration, 19.1 mm similarity registration; right bonobo femur: 39.5 mm

rigid registration, 10.3 mm similarity registration). This was almost double the RMS errors shown in the registration of the tibia and femur of the Spy II bones (5.1 mm to 16.5 mm; Table 1).

Visualisation of the registration of bonobo data to motion data shows the differential morphology of the bonobo lower limb bones in comparison with anatomically modern humans and Neandertals (Figure 5). Full extension of the knee (Figure 5B) clearly shows that there is a joint impeachment, due to an incompatibility of the joint surface morphology in this particular position. Motion simulation seemed to be more natural above about 40 degrees flexion (Figure 5C).

Customised motion representation

The visualisation of the results (Figures 4 and 5) from lhpFusionBox gave an initial qualitative impression of the locomotor ability of Neandertals and bonobos to perform motion tasks in comparison to anatomically modern humans. An estimation of morphological differences was obtained using RMS errors during registration. Further difference quantification was achieved by analysing motion representation from the results of registration of 3D bone models to motion
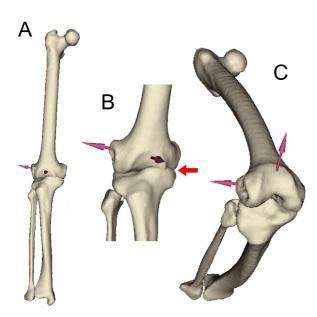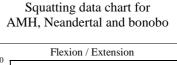
Figure 5. Visualisation of final registration of bonobo data to motion data. A: full skeleton; B: view on the knee joint; C: the skeleton during a squat movement. Joint impeachment is indicated with the horizontal arrow on B.

data. This quantification was performed within lhpFusionBox for the knee joint (Figure 6).

On each joint segment (for the knee: the femur and the tibia) an anatomical reference system (ARS) was attached, using previously palpated ALs. ARS location and orientation were in accordance with the standards recommended by the International Society of Biomechanics (ISB; Wu & Cavanagh, 1995; Wu *et al.*, 2002; Van Sint Jan, 2005). The ARS obtained in this study is visible on Figures 4 and 5, for the Neandertal and bonobo respectively. Note that the axis of flexion-extension shows a similar orientation between all species as the axis was built from ALs located on the femoral condyles which were aligned during spatial registration. OVP (Orientation Vector projected on Proximal AF) was used to express the final motion representation (Woltring, 1994). The method is illustrated on a motion of squatting. Squatting was selected rather than walking because this movement exploits the full range of joint motion. Results of this motion representation between Neandertals, anatomically modern humans and bonobos depict the morphological differences between the three species (Figure 6).

As expected, flexion-extension curves are similar between the three species because the motion axis was oriented using ALs used for registration. Comparison of the motion curve with the ob-

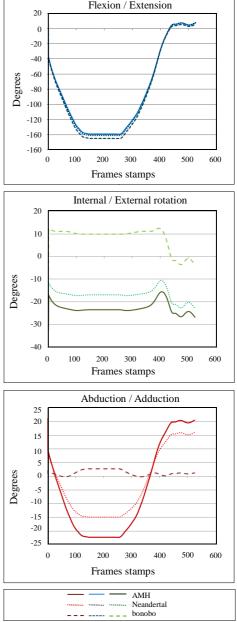Squatting data chart for
AMH, Neandertal and bonobo

Figure 6. Motion representation of Abduction/ Adduction, Internal rotation/External rotation and Flexion/Extension of the knee joint during squatting between anatomically modern humans (AMH), Neandertals and bonobos.

	Dif. AMH – Neandertals			Dif. AMH – Bonobos		
	Flex/Ext	Abd/Add	Int/ExtR	Flex/Ext	Abd/Add	Int/ExtR
Average	1.2	4.8	6.0	3.9	16.6	31.4
Standard deviation	0.8	2.3	1.0	1.7	7.8	4.0
Maximum difference	2.1	7.4	6.7	5.6	25.1	34.4

Table 2. Differences (in degrees) between anatomically modern humans (AMH) and Neandertals (left part of table) and between anatomically modern humans (AMH) and bonobos (right part).

servable joint empeachment (Figure 5B) clearly demonstrates that full knee extension would be difficult for bonobos. This is in agreement with the observation that bonobos typically demonstrate a bent-knee posture during bipedal locomotion of at least 60 degrees flexion and higher (D'Août *et al.*, 2004). There is a large difference between anatomically modern humans and bonobos for the motion representation of the abduction/adduction and internal and external rotation DOFs (Table 2). This indicates that femoral and tibial bone joint morphologies in bonobos differ from both Neandertals and anatomically modern humans.

The comparison of Neandertals with anatomically modern humans demonstrates that differences between motion representations are small. This is due to the fact that the 3 axes of the ARS are oriented in a similar way. This demonstrates that joint orientation is similar between these two hominid groups (Table 2).

DISCUSSION AND CONCLUSIONS

The study aimed to reconstruct a full 3D geometrical lower limb model of a Neandertal using a validated method whilst keeping track of the experimental registration errors (RMS errors) from ALs located at the bone surface. This model was then registered to motion data obtained from a volunteer. All results were displayed in a computer graphics interface for qualitative visual assessment. Motion representation further allowed quantification of morphological similarities. This study focused on the knee joint during a squatting motion, although the entire lower limb model, including pelvis, is now available. The results of the Spy II knee joint registered to motion data of a modern day human seem to demonstrate that this particular individual was capable of performing

the same bipedal motion as anatomically modern humans. A motion requiring a large range of joint motion (such as squatting) was shown to be possible from both a morphological and kinematics point of view. The motion representation demonstrated that the Spy II bones demonstrated slightly more internal/external rotation than humans and slightly less abduction/adduction (Figure 6) although the differences were small and may also be related to experimental artefacts and errors (e.g. during the registration process). In conjunction with a similar motion representation for all DOFs, small RMS errors obtained during the ALs registration indicate that bone morphology and joint orientation of the reconstructed Neandertal were similar to the anatomically modern humans used in this study.

The hypothesis that bonobos have a similar bipedal gait to anatomically modern humans could not be verified in this study. The visualisation of motion reconstruction showed serious discrepancies between joint surface and motion in full extension and appears to demonstrate that the bonobo is physiologically incapable of moving into a fully extended position. The large RMS errors obtained by rigid scaling demonstrate that, as expected, large morphological differences exist between this species and anatomically modern humans. This conclusion indicates that the data processing pipeline presented in this paper seems to succeed in differentiating incompatibility between given bone morphologies, joint geometry and orientation, and given motions.

This study seems to confirm the pattern of other studies on the Neandertal morphology of the lower limb (i.e. Straus Jr & Cave, 1957; Trinkaus, 1983; Trinkaus & Ruff, 1989) in that Neandertals essentially seem to have had a similar bipedal gait to modern humans.

LhpFusionBox is a useful tool in the analysis of fossil locomotion and we aim to further develop the software to specific palaeo-anthropological requirements. Next steps are to register the model to differential motion data obtained from volunteers and to analyse the knee, ankle and hip joints using the newly developed scaling system. Muscle attachment ALs will be integrated on the skeletal material using the method described above and used to simulate and analyse various biomechanical parameters. Supplementary bony ALs will also be used to further validate the method (i.e. ALs on the diaphyseal shafts to measure curvature, internal pelvic ALs, additional points on smaller bones).

We are cautious of accepting the null hypothesis *Neandertals had a similar bipedal gait to anatomically modern humans* outright – however based on the initial results from the knee joint of Spy II we cannot reject this null hypothesis. At this moment we can say that Neandertals seem to have had the skeletal morphology and knee joint surface to enable this particular individual to perform the same bipedal motion as anatomically modern humans. Further research will give greater insights into this question.

ACKNOWLEDGEMENTS

BIBLIOGRAPHY

BAR-YOSEF O., VANDERMEERSCH B., ARENS-BURG B., BELFER-COHEN A., GOLDBERG P., LAVILLE H., MEIGNEN L., RAK Y., SPETH J. D., TCHERNOV E., TILLIER A.-M. & WEINER S., 1992. The excavations in Kebara Cave, Mount Carmel. *Current Anthropology*, **33**: 497-550.

BEN-ITZHAK S., SMITH P. & BLOOM R. A., 1988. Radiographic study of the humerus in Neandertals and *Homo sapiens sapiens*. *American Journal of Physical Anthropology*, **77** (2): 231-242.

BOULE M., 1911. L'homme fossile de La Chapelle-aux-Saints. *Annales de Paléontologie*, **6**: 111-172.

BOULE M., 1912. L'homme fossile de La Chapelle-aux-Saints. *Annales de Paléontologie*, **7**: 85-192.

BOULE M., 1913. L'homme fossile de La Chapelle-aux-Saints. *Annales de Paléontologie*, **8**: 1-70.

BOULE M. & VALLOIS H., 1957. *Fossil Men: A textbook of human palaeontology.* New York, Dryden Press.

CARRIER D. R., KAPOOR A. K., KIMURA T., NICKELS M. K., SATWANTI S. E. C., SO J. K. & TRINKAUS E., 1984. The energetic paradox of human running and hominid evolution. *Current Anthropology*, **25** (4): 483-495.

CHALLIS J. H., 1995. A procedure for determining rigid body transformation parameters. *Journal of Biomechanics*, **26**: 733-737.

D'AOÛT K., VEREECKE E. E., SCHOONAERT K., CLERCQ D. D., VAN ELSACKER L. & AERTS P., 2004. Locomotion in bonobos (*Pan paniscus*): differences and similarities between bipedal and quadrupedal terrestrial walking, and a comparison with other locomotor modes. *Journal of Anatomy*, **204**: 353-361.

FRAIPONT J. & LOHEST M., 1886. La race humaine de Néanderthal ou de Canstadt, en Belgique. Recherches ethnologiques sur des ossements humains, découverts dans des dépôts quaternaires d'une grotte à Spy et détermination de leur âge géologique. Note préliminaire. *Bulletin de l'Académie royale des Sciences de Belgique*, 3ᵉᵐᵉ série, **XII**: 741-784.

FRAIPONT J. & LOHEST M., 1887. La race humaine de Néanderthal ou de Canstadt en Belgique. Recherches ethnologiques sur des ossements humains, découverts dans des dépôts quaternaires d'une grotte à Spy et détermination de leur âge géologique. *Archives de Biologie*, **7**/1886: 587-757.

GRUSS L. T., 2007. Limb length and locomotor biomechanics in the genus *Homo*: An experimental study. *American Journal of Physical Anthropology*, **134** (1): 106-116.

HORN B. K. P., 1987. Closed-form solution of absolute orientation using unit quaternions. *Journal of the Optical Society of America A*, **4**: 629-642.

HRDLIČKA A., 1930. *The skeletal remains of early man*. Smithsonian Miscellaneous Collections, **83**: 379 p.

KAPANDJI I. A., 1985. *Physiologie articulaire - II. Membre inférieur.* Paris, Maloine, 5ᵉᵐᵉ édition.

MILLER J. A. & GROSS M. M., 1998. Locomotor advantages of Neandertal skeletal morphology at the knee and ankle. *Journal of Biomechanics*, **31**: 355-361.

POLK J. D., 2004. Influence of limb proportions and body size on locomotor kinematics in terrestrial primates and fossil hominins. *Journal of Human Evolution*, **47**: 237-252.

RAK Y., 1991. The pelvis. *In*: O. BAR-YOSEF & B. VANDERMEERSCH (ed.), *Le Squelette Moustérien de Kébara 2, Mt. Carmel, Israel*. Paris, CNRS Éditions: 147-156.

RAK Y. & ARENSBURG B., 1987. Kebara 2 Neanderthal iliac: first look at a complete inlet. *American Journal of Physical Anthropology*, **73** (2): 227-231.

RICHMOND B. G. & JUNGERS W. L., 2008. *Orrorin tugenensis* femoral morphology and the evolution of hominin bipedalism. *Science*, **319**: 1662-1665.

RUFF C. B., 2009. Relative limb strength and locomotion in *Homo habilis*. *American Journal of Physical Anthropology*, **138** (1): 90-100.

RUFF C. B., TRINKAUS E., WALKER A. & LARSEN C. S., 1993. Postcranial robusticity in *Homo*. I: temporal trends and mechanical interpretation. *American Journal of Physical Anthropology*, **91** (1): 21-53.

SAWYER G. J. & MALEY B., 2005. Neanderthal reconstructed. *The Anatomical Record Part B: The New Anatomist*, **283B** (1): 23-31.

SCHMITZ R. W., SERRE D., BONANI G., FEINE S., HILLGRUBER F., KRAINITZKI H., PÄÄBO S. & SMITH F. H., 2002. The Neandertal type site revisited: Interdisciplinary investigations of skeletal remains from the Neander Valley, Germany. *Proceedings of the National Academy of Sciences USA*, **99** (20): 13342-13347.

SELLERS W. I., CAIN G. M., WANG W. & CROMPTON R. H., 2005. Stride lengths, speed and energy costs in walking of *Australopithecus afarensis*: using evolutionary robotics to predict locomotion of early human ancestors. *Journal of the Royal Society Interface*, **2**: 431-441.

SELLERS W. I., DENNIS L. A., WANG W.-J. & CROMPTON R. H., 2004. Evaluating alternative gait strategies using evolutionary robotics. *Journal of Anatomy*, **204**: 343-351.

SEMAL P., ROUGIER H., CREVECOEUR I., JUNGELS C., FLAS D., HAUZEUR A., MAUREILLE B., GERMONPRÉ M., BOCHERENS H., PIRSON S., CAMMAERT L., DE CLERCK N., HAMBUCKEN A., HIGHAM T., TOUSSAINT M. & ᴠᴀɴ ᴅᴇʀ PLICHT J., 2009. New Data on the Late Neandertals: Direct Dating of the Belgian Spy Fossils. *American Journal of Physical Anthropology*, **138** (4): 421-428.

SHOLUKHA V., LEARDINI A., SALVIA P., ROOZE M. & VAN SINT JAN S., 2006. Double-step registration of in vivo stereophotogrammetry with both in vitro electrogoniometry and CT medical imaging. *Journal of Biomechanics*, **39** (11): 2087-2095.

STEUDEL-NUMBERS K. L. & TILKENS M. J., 2004. The effect of lower limb length on the energetic cost of locomotion: implications for fossil hominins. *Journal of Human Evolution*, **47** (1-2): 95-109.

STRAUS Jʀ W. L. & CAVE A. J. E., 1957. Pathology and the posture of Neanderthal man. *The Quarterly Review of Biology*, **32** (4): 348-363.

TATTERSALL I. & SCHWARTZ J., 2007. The distinctiveness and systematic context of *Homo neanderthalensis*. *In*: K. HARVATI & T. HARRISON (ed.), *Neanderthals revisited: New approaches and perspectives*. Dordrecht, Springer: 9-22.

TRINKAUS E., 1981. Neandertal limb proportions and cold adaptation. *In*: C. B. STRINGER (ed.), *Aspects of Human Evolution*. London, Taylor & Francis: 187-224.

TRINKAUS E., 1983. *The Shanidar Neandertals*. New York, Academic Press: 502 p.

TRINKAUS E., 1985. Pathology and the Posture of the La Chapelle-aux-Saints Neandertal. *American Journal of Physical Anthropology*, **67** (1): 19-41.

TRINKAUS E., CHURCHILL S. E. & RUFF C. B., 1994. Postcranial robusticity in *Homo*. II: humeral bilateral asymmetry and bone plasticity. *American Journal of Physical Anthropology*, **93** (1): 1-34.

TRINKAUS E., CHURCHILL S. E. & RUFF C. B., 1999. Long bone shaft robusticity and body proportions of the Saint-Césaire 1 Châtelperronian Neanderthal. *Journal of Archaeological Science*, **26**: 753-773.

TRINKAUS E. & RUFF C. B., 1989. Diaphyseal cross-sectional morphology and biomechanics of the Fond-de-Forêt 1 femur and the Spy 2 femur and tibia. *Anthropologie et Préhistoire*, **100**: 33-42.

TRINKAUS E., RUFF C. B. & CHURCHILL S. E., 1998. Locomotion and body proportions of the Saint-Césaire 1 Châtelperronian Neandertal. *Proceedings of the National Academy of Sciences USA*, **95**: 5836-5840.

TRINKAUS E. & SHIPMAN P., 1992. *The Neandertals: Of skeletons, scientists and scandal*. New York, Vintage Books.

VAN SINT JAN S., 2005. Introducing anatomical and physiological accuracy in computerized anthropometry for increasing the clinical usefulness of modeling systems. *Critical Reviews of Physical and Rehabilitation Medicine*, **17** (4): 249-274.

VAN SINT JAN S., 2007. *Color atlas of skeletal landmark definitions; Guidelines for reproducible manual and virtual palpations*. Edinburgh, Churchill Livingstone Elsevier.

VAN SINT JAN S., DEMONDION X., LOURYAN S., CLAPWORTHY G., ROOZE M., COTTEN A. & VICECONTI M., 2006. Multimodal visualisation interface for data management, self-learning and data presentation. *Surgical and Radiological Anatomy*, **28**: 518-524.

13

VAN SINT JAN S., HILAL I., SALVIA P., SHOLUKHA V., POULET P., KIRAKOYA I. & ROOZE M., 2003. Data representation for joint kinematics simulation of the lower limb within an educational context. *Medical Engineering & Physics*, **25** (3): 213-220.

VAN SINT JAN S., SALVIA P., HILAL I., SHOLUKHA V., ROOZE M. & CLAPWORTHY G., 2002. Registration of 6-DOFs electrogoniometry and CT medical imaging for 3D joint modeling. *Journal of Biomechanics*, **35**: 1475-1484.

VEREECKE E. E., D'AOÛT K., PAYNE R. & AERTS P., 2005. Functional analysis of the foot and ankle myology of gibbons and bonobos. *Journal of Anatomy*, **206** (5): 453-476.

VICECONTI M., TADDEI F., MONTANARI L., TESTI D., LEAMIDI A., CLAPWORTHY G. & VAN SINT JAN S., 2007a. Multimod Data Manager: a tool for data fusion. *Computer Methods and Programs in Biomedicine*, **87**: 148-159.

VICECONTI M., ZANNONI C., TESTI D., PETRONE M., PERTICONI S., QUADRANI P., TADDEI F., IMBODEN S. & CLAPWORTHY G., 2007b. The multimod application framework: A rapid application development tool for computer aided medicine. *Computer Methods and Programs in Biomedicine*, **85** (2): 138-151.

WANG W., CROMPTON R. H., CAREY T. S., GUNTHER M. M., LI Y., SAVAGE R. & SELLERS W. I., 2004. Comparison of inverse-dynamics musculo-skeletal models of AL 288-1 *Australopithecus afarensis* and KNM-WT 15000 *Homo ergaster* to modern humans, with implications for the evolution of bipedalism. *Journal of Human Evolution*, **47**: 453-478.

WEAVER T. D., 2003. The shape of the Neandertal femur is primarily the consequence of a hyperpolar body form. *Proceedings of the National Academy of Sciences USA*, **100** (12): 6926-6929.

WOLTRING H. J., 1994. 3-D attitude representation of human joints: a standardisation proposal. *Journal of Biomechanics*, **27**: 1399-1914.

WU G. & CAVANAGH P. R., 1995. ISB recommendations for standardisation in the reporting of kinematic data. *Journal of Biomechanics*, **28**: 257-1261.

WU G., SIEGLER S., ALLARD P., KIRTLEY C., LEARDINI A., ROSENBAUM D., WHITTLE M., D'LIMA D., CRISTOFOLINI L., WITTE H., SCHMID O. & STOKES I., 2002. ISB recommendation on definitions of joint coordinate systems of various joints for the reporting of human joint motion-Part I: ankle, hip, spine. *Journal of Biomechanics*, **35**: 543-548.

AUTHORS AFFILIATION

Tara CHAPMAN
Fedor MOISEEV
Stéphane LOURYAN
Marcel ROOZE
Serge VAN SINT JAN
Laboratory of Anatomy, Biomechanics
and Organogenesis (LABO)
Faculty of Medicine
Université Libre de Bruxelles (ULB)
808, Lennik Street
1070 Brussels
Belgium
tchapman@ulb.ac.be
roozem@ulb.ac.be
fmoiseev@ulb.ac.be
slouryan@ulb.ac.be
sintjans@ulb.ac.be

Tara CHAPMAN
Earth and History of Life
Royal Belgian Institute of Natural Sciences
29, Vautier Street
1000 Brussels
Belgium
tara.chapman@naturalsciences.be

Stéphane LOURYAN
Department of Radiology
ULB Erasmus Hospital
808, Lennik Street
1070 Brussels
Belgium